materials

MDPI

Supplementary Materials

Controlling the Dissolution Behavior of (Meth)acrylate-Based Photoresist Polymers in Tetramethylammonium Hydroxide by Introducing Adamantyl Groups

Jinyoung Kim, Choong-Jae Lee, Dong-Gun Lee, Geon-Ho Lee, Jayoung Hyeon, Yura Choi and Namchul Cho *

Department of Energy Engineering, Soonchunhyang University, 22 Soonchunhyang-ro, Asan 31538, Republic of Korea; kjy1624@sch.ac.kr (J.K.); cndwolee1397@sch.ac.kr (C.-J.L.); alclsro6202@naver.com (D.-G.L.); sinb0603@sch.ac.kr (G.-H.L.); jayoung@sch.ac.kr (J.H.); bnbn3238@sch.ac.kr (Y.C.)

* Correspondence: chon7@sch.ac.kr

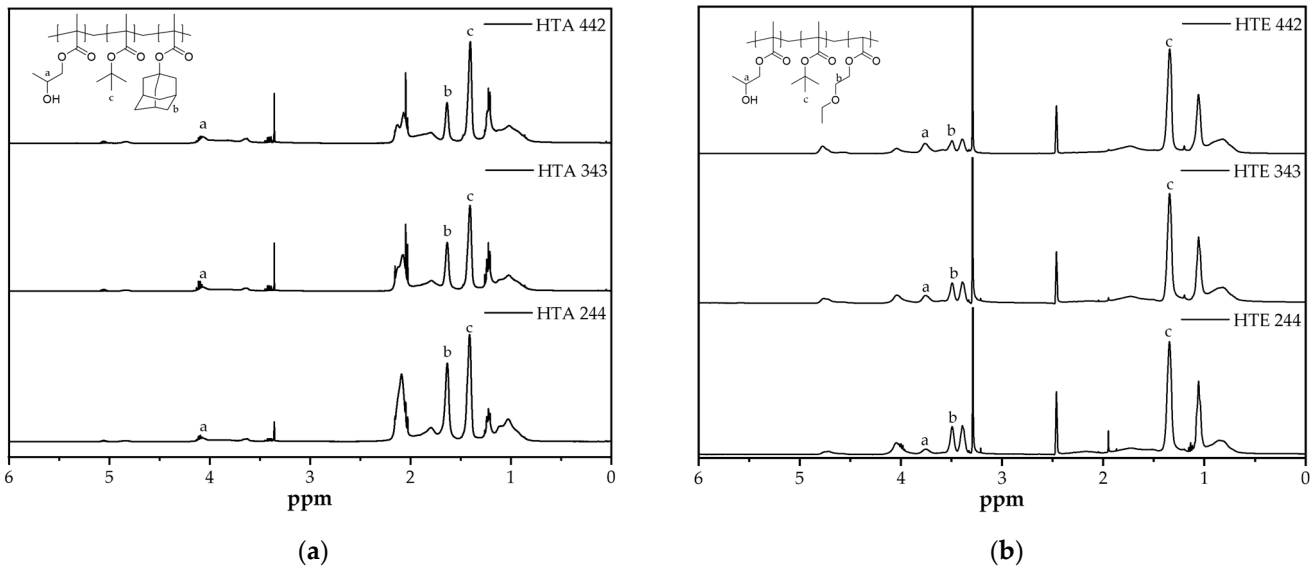


Figure S1. ^{1}H NMR spectra of (a) HTA and (b) HTE polymers.

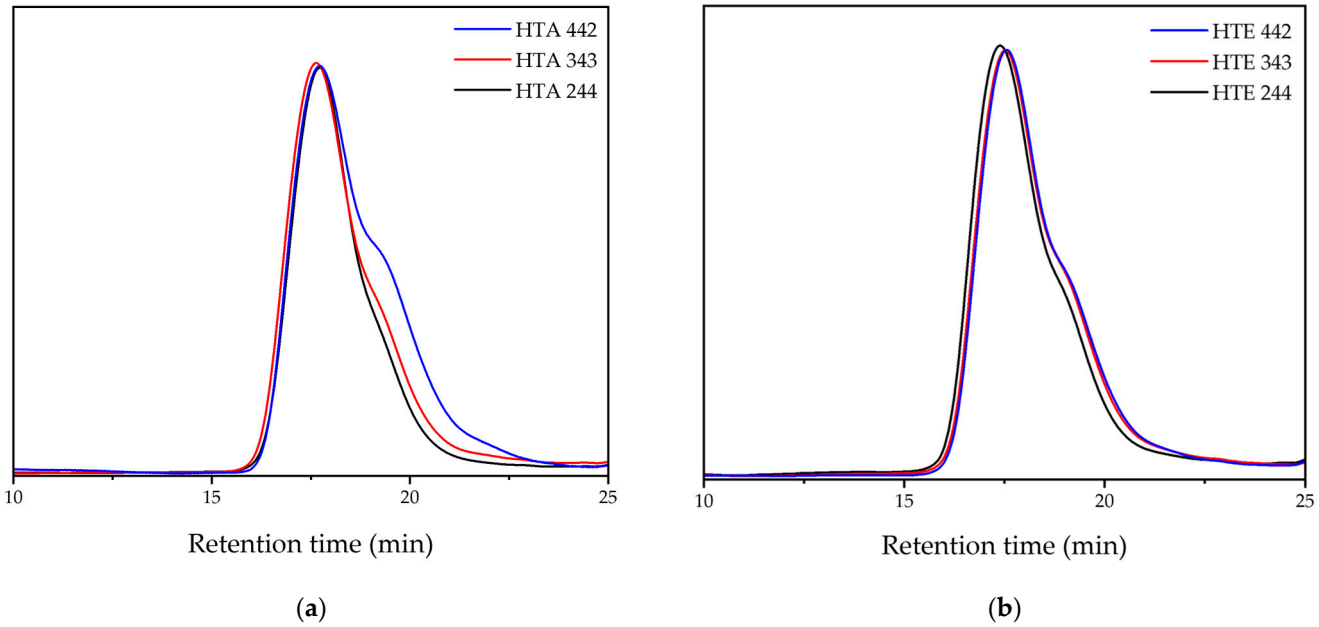


Figure S2. GPC data for the (a) HTA and (b) HTE polymers at various ratios.

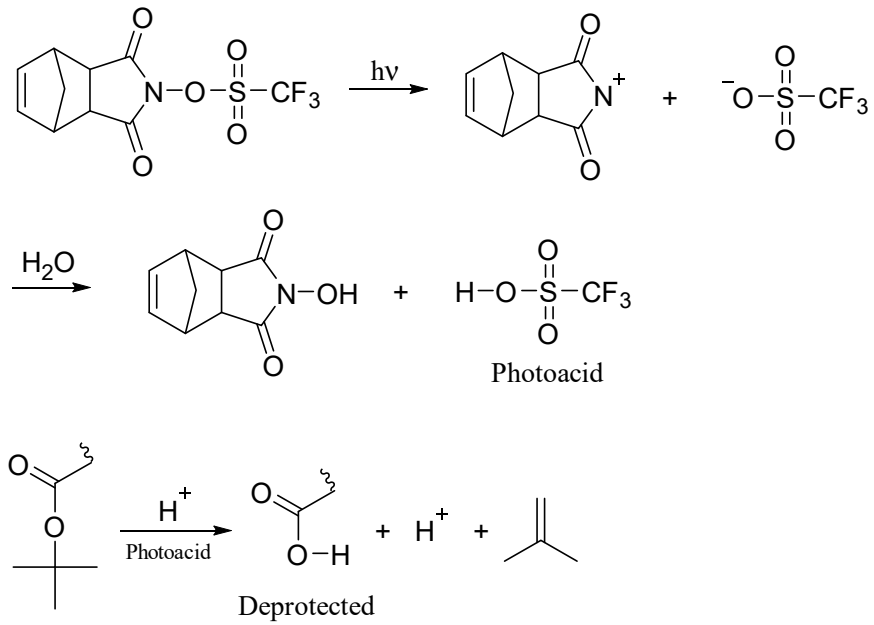


Figure S3. Scheme illustrating the photoacid generation reaction via photolysis of N-((trifluoromethyl sulfonyl)oxy)-5-norbornene-2,3-dicarboximide (NDI) and the deprotection reaction of t-BMA.

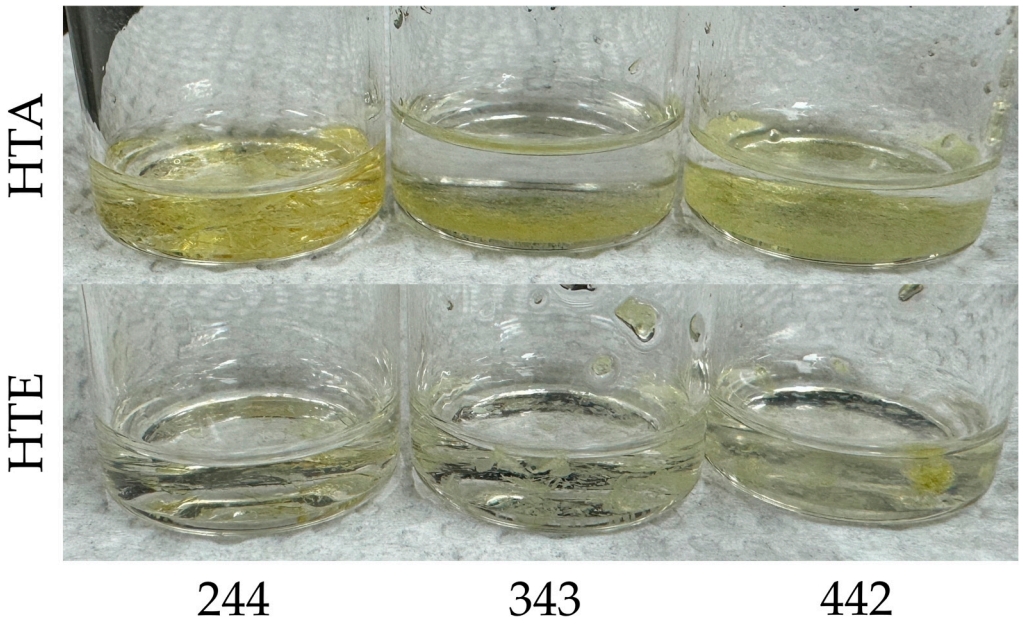


Figure S4. Image of a polymer in PGEMEA solution cross-linked by photoacids upon exposure to light.

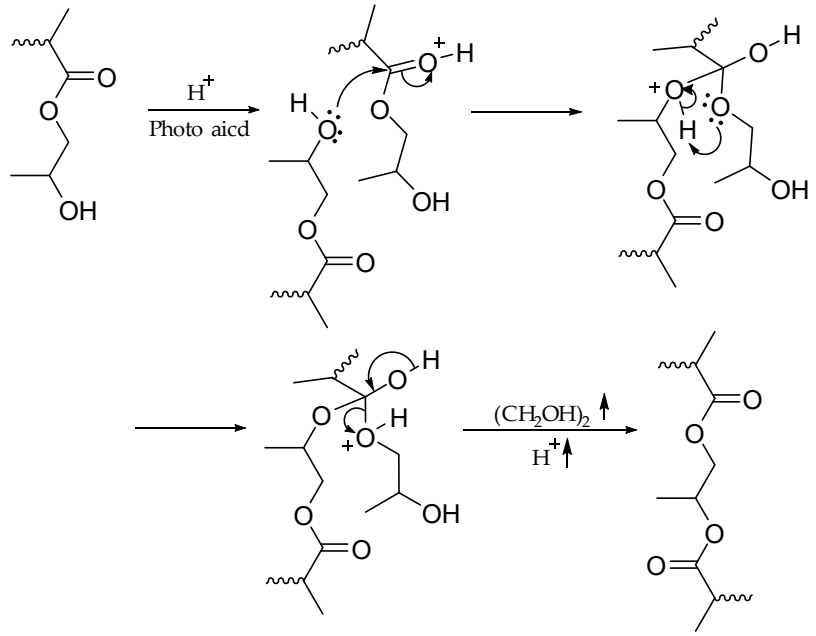


Figure S5. Scheme depicting the cross-linking reaction via transesterification of HPMA by photoacid.

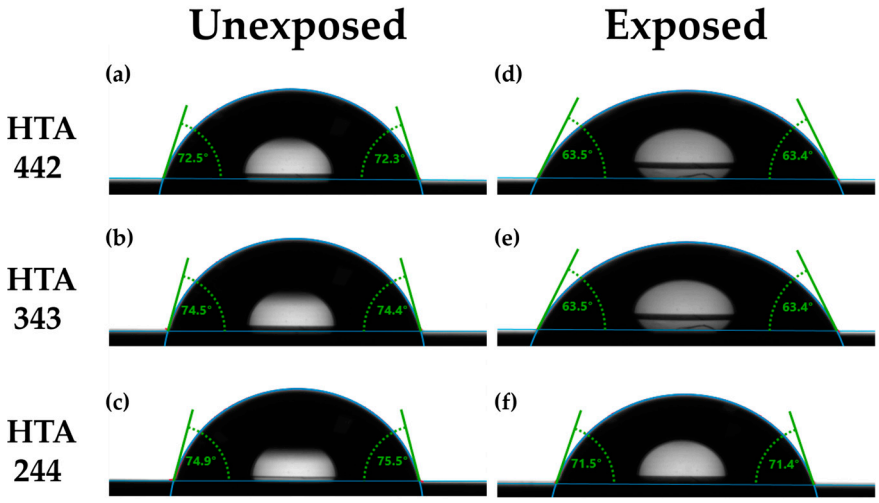


Figure S6. Images of TMAH contact angles on HTA polymer-based photoresist films synthesized at various ratios: (a–c) unexposed HTA 442, 343, and 244 films; (d–f) exposed HTA 442, 343, and 244 films.

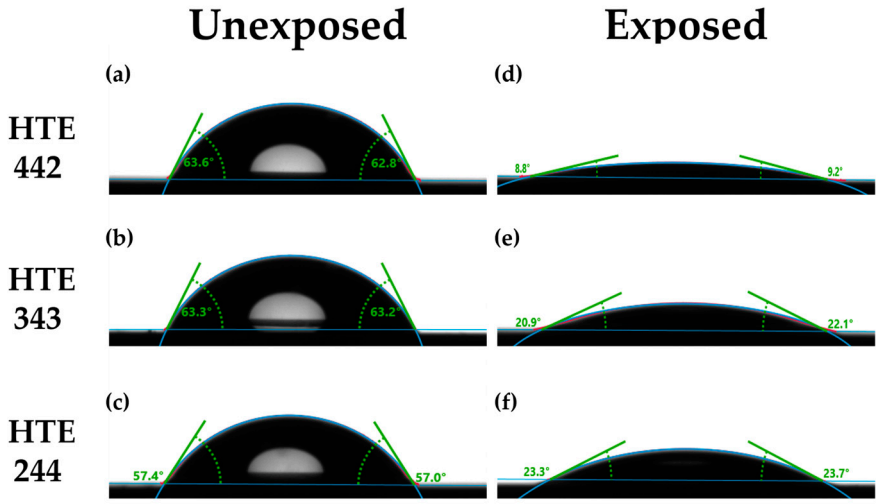


Figure S7. Images of TMAH contact angles on HTE polymer-based photoresist films synthesized at various ratios: (a–c) unexposed HTE 442, 343, and 244 films; (d–f) exposed HTE 442, 343, and 244 films.

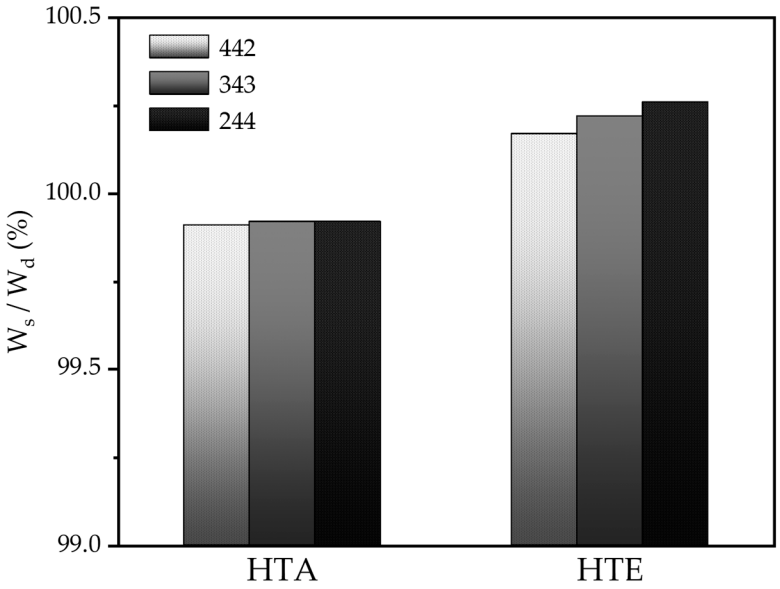


Figure S8. Graph of weight ratio (W_s / W_d) of HTA and HTE polymer-based films obtained through TMAH immersion.